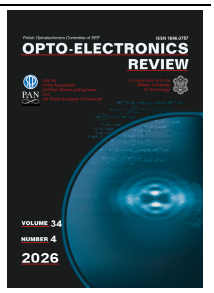
Opto-Electronics Review

journal homepage: publishinghouse.pan.pl/opelre



Multispectral fibre-optic reflectometer with extended UV-VIS-NIR LEDs for non-destructive classification of eggshell optical signatures associated with *Mycoplasma synoviae*

Anna Pakuła[1*], Sławomir Paśko[1], Piotr Bacciarelli-Grobelny[1], Andrzej Stach[1], Szymon Rudnicki[1], Paweł Marć[2], Olimpia Kursa[3]

[1] Institute of Micromechanics and Photonics, Warsaw University of Technology, ul. św. Andrzeja Boboli 8, 02-525 Warsaw, Poland
[2] Faculty of New Technologies and Chemistry, Military University of Technology, ul. gen. Sylwestra Kaliskiego 2, 00-908 Warsaw, Poland
[3] Department of Poultry Diseases, National Veterinary Research Institute, Al. Partyzantów 57, 24-100 Puławy, Poland

Article info

Article history:
Received 01 Jul. 2026
Received in revised form 10 Sep. 2026
Accepted 22 Sep. 2026
Available online 06 Nov. 2026

Keywords:
multispectral reflectometer;
machine learning classification;
Mycoplasma synoviae.

Abstract

This paper presents the development and evaluation of the multispectral fibre-optic reflectometer expanded to the UV-VIS-NIR spectral range for the non-destructive classification of eggshell originating from healthy or *Mycoplasma synoviae* (MS) infected poultry. MS is a highly contagious pathogen causing significant economic losses, particularly by altering the structure and reflectance of eggshells. The multispectral fibre-optic reflectometer (MFOR) system evaluates back-reflected light using machine learning algorithms to accurately classify eggshells as originating from healthy or MS infected hens. In this study, four categories of eggshells (brown/white, infected/healthy) were tested using different LED combinations across an extended wavelength spectrum. The machine learning classification model achieved exceptional precision, identifying the optimal wavelength combinations as 340, 490, and 660 nm for white eggs (mean F-score = 0.998) and 340, 490, and 560 nm for brown eggs (mean F-score = 1.000). These findings suggest that incorporating UV wavelengths enhances the MFOR ability to rapidly and non-invasively diagnose MS in a flock based on eggshell optical properties.

1. Introduction

The multispectral fibre-optic reflectometer (MFOR) was developed for non-destructive measurements of various biological objects. It was successfully tested for classifying whether eggs originated from healthy hens or those infected with *Mycoplasma synoviae* (MS), based on eggshell reflectance measurements [1–4].

The system has two key components: selected LEDs with varied spectral characteristics and machine learning algorithms that support analyses of interrelationships among reflectance losses for the used LEDs.

In the previous MFOR design, six selected LEDs from the VIS spectrum, ranging from 413 nm to 699 nm were used. This configuration allowed for differentiating between eggs laid by healthy and infected birds with an F-score greater than 0.9 [2]. Given these possibilities, the most critical parameter for each use case is selecting LEDs to cover the required spectral range. Therefore, expanding the wavelength range to include both UV and NIR spectra allows us to determine how reflectance losses in these regions influence the system classification capabilities.

MS is a major avian pathogen responsible for infectious synovitis and severe respiratory tract infections. Beyond these clinical manifestations, MS exerts a devastating economic impact on the table egg industry by inducing eggshell apex abnormalities (EAA) syndrome. EAA is characterised by altered calcification processes in the oviduct, leading to eggshells that are thinned, roughened, translucent, and highly prone to cracking. In severe field

*Corresponding author at: anna.pakula@pw.edu.pl

https://doi.org/10.24425/opelre.2026.7669
1896-3757/ Association of Polish Electrical Engineers (SEP) and Polish Academy of Sciences (PAS). Published by PAS
© 2026 The Author(s). This is an open-access article under the CC BY license (https://creativecommons.org/licenses/by/4.0/).

outbreaks, this syndrome can affect up to 24.5% of eggs produced, directly reducing their market value and causing an overall drop in egg production of approximately 5–11%.

Current diagnostic strategies for MS primarily rely on conventional culture methods, serological assays (such as ELISA) [5–8], and molecular techniques such as real-time polymerase chain reaction (PCR) [9–11] or loop-mediated isothermal amplification (LAMP) [12–14]. While molecular tests offer high sensitivity and remain the gold standard, they require specialised laboratory equipment, skilled personnel, and ultimately, the destruction of the sample. Furthermore, classical pathogen isolation is extremely time-consuming, taking up from 21 to 28 days. Consequently, the poultry industry increasingly demands rapid, non-destructive, point-of-care diagnostic tools that can screen flocks directly on the farm [1–5].

Optical methods present a highly promising alternative for the rapid identification of changes induced by MS. Previous studies utilising advanced imaging techniques, such as full-field optical coherence tomography, have revealed profound structural changes in infected eggshells, including a drastic reduction in the number of pores and the absence of the papillary layer in the calcification zone [4]. Building on these distinct optical differences, the MFOR utilises specific light reflectance patterns to distinguish between eggs originating from healthy and MS infected hens. By applying machine learning algorithms to reflectance data, this non-invasive approach can automate and accelerate MS detection, bypassing the limitations of traditional laboratory diagnostics and facilitating early intervention.

2. Multispectral fibre-optic reflectometer with extended UV-VIS-NIR LEDs

2.1. *Setup description*

For tests reported in this paper, four versions of optoelectronic units were built, i.e., three named multispectral AI (MSA) and one benchtop (Benchtop). Among the MSAs, two of them have a 19-inch rack housing which, in this paper, are referred to as MSA 0 and MSA 1. The third optoelectronic unit has a smaller housing and is dedicated to measurements in the UV spectral range; therefore, it is named MSA UV. The benchtop optoelectronic unit has an integrated detection module. An image of all optoelectronic units is shown in Fig. 1. The developed devices differ in the number of LED modules – one, two, or three modules. Each LED module consists of eight LEDs with different spectral characteristics.



Fig. 1. Optoelectronic units used in the MFOR.

Table 1 shows the central wavelengths of each LED. Compared with previous research, the LEDs spectral coverage was substantially extended into the UV and NIR regions.

Light from each optoelectronic module is connected via a fibre-optic bundle to the optical measuring head. Two different fibre bundles were used during experiments. Both are commercially available 1-to-7 fan-out fibre-optic bundles purchased from Thorlabs. The selected bundles had a 600-micron silica core diameter cladded with hard TECS polymer, a 0.39 numerical aperture, and varying spectral characteristics related to high or low concentrations of OH ions in the silica core.

For the reported studies, the spectral region from UV radiation around 350 nm to NIR around 900 nm is of particular interest. Based on the spectral attenuation data provided by the manufacturer, high OH-doped silica is preferable for the MSA UV. Therefore, in Table 1, the central wavelengths of the LEDs used in MSA UV were measured in both types of optical fibre bundles.

Table 1.
Central LED wavelengths of each tested LED module of each optoelectronic unit used in the MFOR[a].

Module indicator	L1 [nm]	L2 [nm]	L3 [nm]	L4 [nm]	L5 [nm]	L6 [nm]	L7 [nm]	L8 [nm]
Benchtop A	856	750	695	657	605	533	506	413
Benchtop B	750	669	667	604	534	466	432	389
MSA 0 A	590	574	561	545	436	403	396	375
MSA 0 B	520	511	495	455	437	404	397	376
MSA 0 C	682	645	597	590	544	509	448	397
MSA 1 A	833	778	742	681	662	627	613	561
MSA 1 B	740	610	574	520	493	435	402	375
MSA 1 C	805	779	662	597	575	544	494	403
MSA UV	368	348	319	297	363	349	323	299

[a] all measurements were done using the fibre optic spectrometer AvaSpec-3648-USB2 (Avantes).

Main parts of the demonstrator version of the MFOR system are shown in Fig. 2 and include: optoelectronic unit (Benchtop, MSA 0, MSA 1, or MSA UV), detection module, fibre-optic bundle, optical head with holders, and a PC with proper software. In the background of that image, optoelectronic units are set up. Each optoelectronic unit is connected to the PC via a USB port, which serves as a power supply and data transfer channel. PC software allows setting up parameters for measurement procedures. Input fibres 2 through 7 of each fibre-optic bundle [as shown in Fig. 3(b)] are directly connected to the selected LEDs in each optoelectronic unit, and the combined output fibre is connected to each optical head. Centre input fibre [marked as 1 in Fig. 3(b)] is connected to a detection module [Fig. 3(a)] and allows for the measurement of a back-reflected signal. Each optical measuring head and holder allows proper positioning of the biological sample for testing. In each optical measuring head, a fibre collimator has been installed, which provides a uniform spot size of approx. 5 millimetres. The collimator main purpose is to focus the maximum amount of back-reflected light into the centre fibre. In Fig. 2, reference objects (ping-pong balls) were placed to calibrate the device.

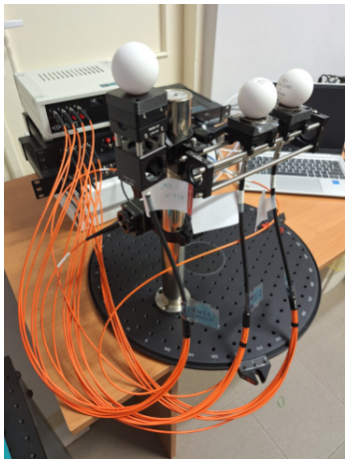


Fig. 2. Multispectral fibre-optic reflectometer (MFOR) with three optical heads and holders, fibre bundles, and MultiSpectrAI (MSA) optoelectronic units.

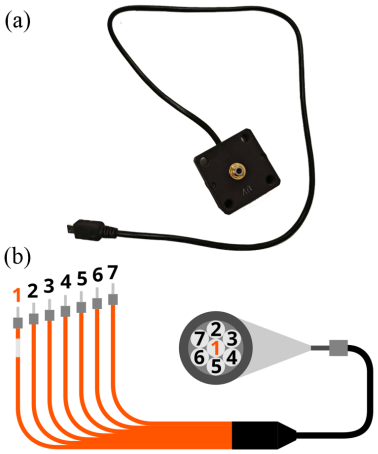


Fig. 3. (a) Detection module with micro-USB cable. (b) Schematic of fibre-optic bundle. The centre fibre marked as 1 is also marked by a white sticker close to its connector.

2.2. Tested samples and measurement procedure

The healthy eggshells were sourced from the internal reference flock of the Department of Poultry Diseases at the National Veterinary Research Institute (NVRI) in Puławy, Poland. Conversely, the MS-changed eggs were obtained from commercial flocks operating under the veterinary supervision of the NVRI. The MS infection status of these commercial flocks was rigorously confirmed using three molecular techniques: specific MS PCR, LAMP, and sequencing of the *vlhA* gene. Prior to the optical measurements, all samples underwent a standardised preparation procedure which included breaking the eggs, rinsing the shells under a stream of tepid, running water, and leaving them to dry for three days.

The measurement procedure aimed to build a comprehensive machine learning dataset, which required an extensive number of data points. The eggshell samples were divided into four categories: brown infected, brown healthy, white infected, and white healthy. Since eggshells originating from MS-infected hens are characterised by structural anomalies such as shell thinning, increased translucency, and extreme fragility, it was strictly necessary to select samples large enough to allow for multiple measurements at distinct spots without structural failure. A comparison between different eggshells from infected hens is shown in Fig. 4.

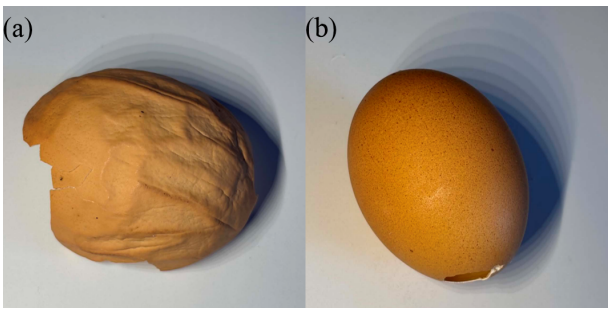


Fig. 4. Exemplary MS-affected shells. (a) Eggshell with visible changes. (b) Eggshell without clearly visible changes.

The measurement series aims to build a machine learning dataset, so it must be relatively large. It was assumed that at least 250 measurements for each LED are required to achieve good machine learning results. The samples, eggshells, were divided into four categories: brown infected, brown healthy, white infected, and white healthy. From each category, 12 eggshells were selected and measured across 21 distinct locations, yielding 252 measurements per LED. Since MS-affected shells exhibit high spatial non-uniformity (as illustrated in Fig. 4), treating measurements from different surface spots as independent data points is well justified. Furthermore, because eggshells are fragile, particularly the infected ones, we selected only those large enough to allow measurements at distinct spots.

During one measurement, 8 LEDs in a module turn on in sequence for 2 milliseconds. The photodiode in the detection module is synchronised with the optoelectronic unit so that the back-reflected signal can be associated with the respective LED. The output value is an average of 10 measurements taken by the photodiode within 2 milliseconds when the LED is turned on. After one sequence, there is a 10-millisecond pause, and the process repeats nine more times, for a total of 10 measurements per diode. The results from each sequence are saved in a .json file.

One series of measurements consists of measuring one category with one LED module, first with LEDs 1 through 6 and then with LEDs 3 through 8, since the fibre-optic bundle allows only 6 input LEDs at a time. Each series of measurements is preceded by a reference measurement using white, uniform ping-pong balls, as shown in Fig. 2. This eliminates any influence from LEDs with different illumination powers and back reflections from the collimator.

3. Experimental results and analysis

3.1. Experimental data preparation

To simplify the analysis, data from diodes of the same manufacturer type, which were located across different devices but had very close measured wavelengths (spread

up to 10 nm), were assumed to come from a single diode. The wavelength value used in further analysis is the manufacturer-specified dominant value in the groups to which a diode is assigned. In most cases, it is equal to the manufacturer-specified wavelength of all diodes in this group.

The data were pre-processed in Python. For each wavelength in a single file, the mean of 10 readings was calculated and then treated as the single measurement result.

The measurement data were normalised using the reference measurements taken during data gathering.

3.2. *Data analysis*

As light from eggshells in a single trial was reflected from slightly offset points on the eggshell, measurements for each wavelength can be treated separately. For each module, data from all diodes were aggregated for both healthy (H) and infected (I) hens' eggshells, both for white and brown colours.

Wavelengths with the greatest separation between H and I measurements were expected to be most effective in the classification algorithm. Therefore, 3 wavelengths with the smallest value of the overlap coefficient (OVL) were chosen for each module. In this case of empirical data points, it was necessary first to apply a continuous kernel density estimation. It was obtained by aggregating normal distribution representations around each relative intensity value, with standard deviation scaled using Silverman's rule of Thumb. Using this procedure, 27 diodes (3 for each of the 9 modules) for both white and brown eggs were selected. Since some of the wavelengths were repeated in different triples, 19 and 21 unique wavelengths were selected for white and brown eggs, respectively. Among these, 13 values were common for both colours and were taken for further analysis (Table 2).

Table 2.
Unique LED wavelengths selected for white and brown eggs.

[nm]	645	525	660	405	430	560	570
	575	590	340	490	365	750	

In order to identify the best small set of wavelengths, the performance of the machine learning classification algorithm was compared across all combinations of 3 of these wavelengths. For each wavelength, separately for each colour, all normalised measurements (from all diodes classified to this wavelength) were assigned as a list of data. For each set of 3 wavelengths, the lists were trimmed to the length of the list corresponding to the wavelength with the fewest readings by randomly removing data from the longer lists, separately for infected and healthy eggshells. For each triple, the following training and scoring procedure was conducted 100 times (in a loop, see Fig. 5) in the KNIME 5.5.0 software. Randomly chosen 70% of data was used for training of the self-organising tree algorithm (SOTA) model [15], which learned to classify eggs into the H and I categories (for a given colour). The remaining 30% of the data was used to evaluate model performance across the three wavelengths. The above procedure was repeated independently for both white and brown eggshells.

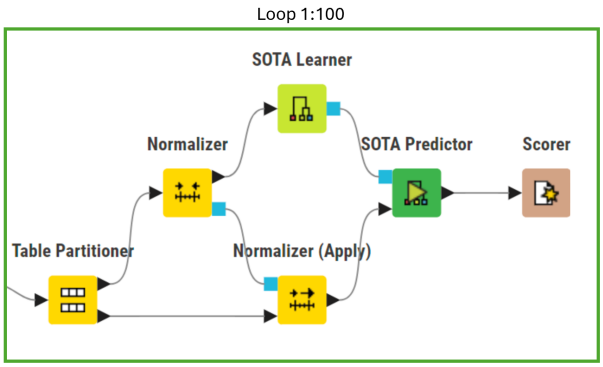


Fig. 5. Data processing workflow used to train and evaluate the SOTA algorithm for one wavelength set. The procedure was repeated independently for all wavelength sets.

The algorithm performance was evaluated based on the F-score. It is obtained from the number of true positives (TP), true negatives (TN), false positives (FP), and false negatives (FN). The Recall variable is introduced as Recall = TP/(TP + FN). The Precision variable is introduced as Precision = TP/(TP + FP). F-score is the harmonic mean of Recall and Precision.

F-score was obtained for classification of H and I eggs, for 100 iterations of training for each triple. For comparison with other triples, the mean of F-scores for I and H across these iterations are computed. The overall score of a triple of wavelengths is computed as a geometric mean of these average F-scores.

It was then possible to sort wavelength triples by their overall score to identify which combinations best distinguish H and I eggs. Data for wavelength sets, their respective F-scores for H and I, and geometric means of F-scores are available upon request. The top overall score was obtained with wavelengths of 340, 490, 660 nm (mean F-score = 0.998) for white eggs and of 340, 490, 560 nm (mean F-score = 1.000) for brown eggs. Combined, they form a wide range of wavelengths (340 – UV/violet, 490 – blue-green, 560 – yellow-green, 660 – red) using four diodes. The second set, with exceptionally strong classification performance, was 430, 570, 660 nm (mean F-score = 0.991) and 430, 560, 660 nm (mean F score = 0.990) for white, and 430, 560, 570 nm (mean F-score = 1.000) for brown eggs.

4. Discussion

While the preliminary results demonstrate the potential of the proposed optical method, several limitations must be acknowledged to properly contextualise the findings and guide future development.

First, a potential source of data bias stems from the origin and heterogeneity of the egg samples. Since this study was exploratory, the reference control group comprised healthy eggs obtained from the National Veterinary Research Institute, whereas the infected samples originated from commercial flocks. Consequently, external confounding variables, such as differences in flock species/breed, dietary regimes, and housing environments, could contribute to the observed spectral variations alongside the biological indicators of infection. Confirming the full robustness and specificity of the classification model will require extensive validation on highly homogeneous flock

populations maintained under standardised environmental and nutritional conditions.

Second, regarding the data partitioning strategy, the current evaluation employed a random 70/30 train-test split based on individual spectral readings. This approach aligns with our core premise of examining localised optical properties across specific shell sections. However, treating individual spot measurements as independent samples may introduce data leakage when evaluating performance at the whole-egg or whole-flock level. For real-world commercial deployment (e.g., automated sorting on production lines), a rigorous leave-one-group-out (LOGO) or leave-one-flock-out cross-validation scheme must be applied. This will ensure that the model accurately generalises to completely unseen batches and individual units.

Finally, transitioning from measuring eggshell fragments to whole eggs should not require changes to the MFOR system, as the light does not penetrate the eggshell deeply enough for backscattered light from inside the egg to influence the measurement. The problem, however, is of a logistical nature, as whole eggs, whose health status is fully characterised, are not easy to obtain – current methods of detecting MS require cracking the egg. Securing such fully documented and traceable egg batches will be essential to establish standardised measurement protocols before scaling the system for high-throughput industrial applications.

5. Conclusions

In conclusion, MS infection is one of the most serious challenges for the modern poultry industry, causing massive economic losses primarily through damage to eggshell structure (EAA syndrome) and an overall drop in egg production. Although traditional diagnostic methods, such as time-consuming microbiological culture or sensitive molecular techniques, form the basis of flock monitoring, they have significant limitations. The need to transport material to specialised laboratories, the long turnaround time for results, and the fact that this process involves the irreversible destruction of the sample often prevent a rapid response under field conditions.

In response, the MFOR emerges as a breakthrough solution, enabling immediate, automated, and completely non-destructive detection of MS-changed eggs based on the optical properties of eggshells. By utilising specific light reflectance patterns extended with optimal combinations of wavelengths from the UV-VIS-NIR range (e.g., 340, 490, and 660 nm) and advanced machine learning algorithms, the MFOR allows eggs to be classified as originated from healthy or MS-infected hens with near-flawless precision (F-score close to 1.000). This device facilitates routine screening directly on the farm, bypassing the costs and delays of traditional laboratory diagnostics, which in turn allows for immediate intervention and a drastic reduction in production losses.

Authors' statement

Research concept and design, A.P., S.P., P.M.; collection and/or assembly of data, P.B.G., A.S, S.R.; data analysis and interpretation, S.P., P.B.G.; writing the article, A.P., S.P., P.B.G, A.S., S.R., O.K., P.M.; critical revision of the article, A.P., P.M.; final approval of article, A.P.

Acknowledgements

This project has received funding from the research and innovation budget of the Institute of Micromechanics and Photonics, Warsaw University of Technology. This work was supported by the Program of the Republic of Poland, Research Grant MUT project no. UGB 531-000097-W900-22.

References

[1] Pakuła, A., Paśko, S., Marć, P., Kursa, O. & Jaroszewicz, L. R. AI classification of eggs' origin from *Mycoplasma synoviae*-infected or non-infected poultry via analysis of the spectral response. *Appl. Sci*. **13**, 12360 (2023). https://doi.org/10.3390/app132212360

[2] Pakuła, A. *et al*. Multispectral portable fibre-optic reflectometer for the classification of the origin of chicken eggshells in the case of *Mycoplasma synoviae* infections. *Sensors* **22**, 8690 (2022). https://doi.org/10.3390/s22228690

[3] Pakuła, A., Paśko, S., Kursa, O. & Komar, R. Reflected light spectrometry and AI-based data analysis for detection of rapid chicken eggshell change caused by *Mycoplasma Synoviae*. *Appl. Sci*. **11**, 7799 (2021). https://doi.org/10.3390/app11177799

[4] Kursa, O., Pakuła, A., Tomczyk, G., Paśko, S. & Sawicka, A. Eggshell apex abnormalities caused by two different *Mycoplasma synoviae* genotypes and evaluation of eggshell anomalies by full-field optical coherence tomography. *BMC Vet. Res*. **15**, 1 (2019). https://doi.org/10.1186/s12917-018-1758-8

[5] Lazcka, O., Campo, F. J. D. & Muñoz, F. X. Pathogen detection: A perspective of traditional methods and biosensors. *Biosens. Bioelectron.* **22**, 1205–1217 (2007). https://doi.org/10.1016/j.bios.2006.06.036

[6] Feberwee, A., de Vries, T. S. & Landman, W. J. M. Seroprevalence of *Mycoplasma synoviae* in Dutch commercial poultry farms. *Avian Pathol.* **37**, 629–633 (2018). https://doi.org/10.1080/03079450802484987

[7] Itoh, S. *et al*. New rapid enzyme-linked immunosorbent assay to detect antibodies against bacterial surface antigens using filtration plates. *Biol. Pharm. Bull*. **25**, 986–990 (2002). https://doi.org/10.1248/bpb.25.986

[8] Galikowska, E. *et al*. Specific detection of Salmonella enterica and *Escherichia coli* strains by using ELISA with bacteriophages as recognition agents. *Eur. J. Clin. Microbiol. Infect. Dis*. **30**, 1067–1073 (2011). https://doi.org/10.1007/s10096-011-1193-2

[9] Hong, Y. *et al*. Specific detection and typing of *Mycoplasma synoviae* strains in poultry with PCR and DNA sequence analysis targeting the hemagglutinin encoding gene *vlhA*. *Avian Dis*. **48**, 606–616 (2004). https://doi.org/10.1637/7156-011504r

[10] Hammond, P. P., Ramírez, A. S., Morrow, C. J. & Bradbury, J. M. Development and evaluation of an improved diagnostic PCR for *Mycoplasma synoviae* using primers located in the haemagglutinin encoding gene *vlhA* and its value for strain typing. *Vet. Microbiol*. **136**, 61–68 (2009). https://doi.org/10.1016/j.vetmic.2008.10.011

[11] Fraga, A. P. *et al.* A multiplex real-time PCR for detection of Mycoplasma gallisepticum and Mycoplasma synoviae in clinical samples from Brazilian commercial poultry flocks. *Braz. J. Microbiol.* **44**, 505–510 (2013). https://doi.org/10.1590/s1517-83822013000200028

[12] Kursa, O., Woźniakowski, G., Tomczyk, G., Sawicka, A. & Minta, Z. Rapid detection of *Mycoplasma synoviae* by loop-mediated isothermal amplification. *Arch. Microbiol*. **197**, 319–325 (2014). https://doi.org/10.1007/s00203-014-1063-2

[13] Kursa, O., Tomczyk, G. & Sawicka, A. Prevalence and phylogenetic analysis of Mycoplasma synoviae strains isolated from Polish chicken layer flocks. *J. Veter. Res*. **63**, 41–49 (2019). https://doi.org/10.2478/jvetres-2019-0010

[14] Joung, J. *et al*. Deep learning optical spectroscopy based on experimental database: Potential applications to molecular design. *JACS Au* **1**, 427–438 (2021). https://doi.org/10.1021/jacsau.1c00035

[15] Dopazo, J. & Carazo, J. Phylogenetic reconstruction using an unsupervised growing neural network that adopts the topology of a phylogenetic tree. *J. Mol. Evol*. **44**, 226–233 (1997). https://doi.org/10.1007/PL00006139